Polymer 52 (2011) 3175–3182

Contents lists available at ScienceDirect

Polymer

journal homepage: www.elsevier.com/locate/polymer

Dynamics near the filler surface in natural rubber-silica nanocomposites

Daniel Fragiadakis [a,*], Liliane Bokobza [b], Polycarpos Pissis [a]

[a] Department of Physics, National Technical University of Athens, Zografou Campus, 15780 Athens, Greece
[b] Laboratoire PPMD, ESPCI, 10 rue Vauquelin, 75231 Paris Cedex, France

ARTICLE INFO

Article history:
Received 9 March 2011
Received in revised form
12 April 2011
Accepted 21 April 2011
Available online 1 May 2011

Keywords:
Nanocomposite
Glass transition
Molecular dynamics

ABSTRACT

We study the effect of *in situ* synthesized 10 nm silica nanoparticles on the glass transition and dynamics of natural rubber networks using differential scanning calorimetry, broadband dielectric relaxation spectroscopy and thermally stimulated depolarization currents. Even in the absence of specific polymer-filler interactions, polymer segments within a few nanometers of the filler particles exhibit relaxation times up to 2–3 orders of magnitude slower and reduced heat capacity increment at the glass transition compared to bulk natural rubber. These effects are only observed when the nanoparticles are uniformly distributed in the polymer matrix.

1. Introduction

Polymers containing nanoparticles such as nanoscale silica, layered silicates or carbon nanotubes have attracted a lot of interest both from the point of view of applications and that of fundamental polymer science [1–5]. Even for relatively low amounts of nanoparticles, a significant fraction of the polymer is within a distance of several nanometers of the particle surface; this interfacial polymer has potentially different structural and dynamic properties than the bulk. Therefore, nanocomposites may have properties, or combinations of properties, that cannot be obtained for the corresponding bulk polymer or conventional macro- or micro-composites [6].

From a more general point of view, nanocomposites can be used to investigate the fundamental question: what is the effect of proximity to a solid surface on the glass transition and dynamics of polymers? In particular, is there a significant effect at all, and if so, what is its nature and how far from the surface does it extend? There is substantial literature that addresses these issues by studying the dynamics of ultrathin polymer films as well as liquids and polymers confined in various types of porous media [7]. Due to their very large surface to volume ratio, polymer nanocomposites can provide complementary information on the modification of dynamics near particle surfaces.

After more than a decade of research on the dynamics of nanocomposites, the experimental picture is still far from clear. In some cases, the nanoparticles have no effect at all on dynamics, even in well-dispersed composites [8]. In other cases, typically with thermoplastics such as polystyrene and PMMA containing oxide nanoparticles, even very small particle concentrations cause large drop in T_g [9]; this would indicate a strong and long-range effect (tens or even hundreds of nanometers) which has been related to the T_g reduction in ultrathin polymer films [10], however at least in some cases it has been found that this T_g decrease can be removed by annealing [11]. Finally in several studies, a very thin layer (a few nanometers) of interfacial polymer with restricted mobility is detected around the filler particles, while the rest of the polymer follows bulk dynamics [12–21]. This behavior has been described in terms of three-layer models [16–18], two-layer models [14,15,19,20] or a continuous distribution of glass transition temperatures as a function of distance from the particle surface [21].

It has also become evident that one must take care to distinguish a genuine physical change of dynamics due to the presence of nanoparticles, from those changes caused indirectly through other effects. These include, for example, changes in crystallinity, and changes in molecular weight or degree of crosslinking when the polymerization is carried out in the presence of the nanoparticles. In dynamic mechanical measurement, changes in the real part of the shear modulus or to the flow properties can lead to apparent shifts in the mechanical tan δ peak or the appearance of a second loss tangent peak, respectively, even if segmental dynamics remains unchanged [22–24].

* Corresponding author. Present address: Naval Research Laboratory, Chemistry Division, Code 6120, Washington, DC 20375-5342, USA.
E-mail address: daniel.fragiadakis.ctr@nrl.navy.mil (D. Fragiadakis).

0032-3861/$ – see front matter © 2011 Elsevier Ltd. All rights reserved.
doi:10.1016/j.polymer.2011.04.045

Proper dispersion of the nanoparticles in the polymer matrix is crucial, and experimentally challenging since nanoparticles have an extremely strong tendency to aggregate [25]. One approach that has been successful for preparing well-dispersed nanocomposites is sol–gel synthesis of the nanoparticles *in situ* within the polymer matrix. By varying the reaction conditions, one can control the size, dispersion and surface characteristics of the nanoparticles [26]. We have previously studied series of sol–gel derived polydimethylsiloxane (PDMS)-silica and PDMS-titania nanocomposites [12,13,27–30], where PDMS chains interact strongly with the particle surface via hydrogen bonds. PDMS is semicrystalline, and the nanoparticles were found to significantly decrease crystallinity. Taking that into account, we determined that a layer of polymer with a thickness of 2–3 nm (decreasing with increasing temperature) around the silica particles exhibits modified dynamics: decreased heat capacity increment of the calorimetric glass transition, and 3–5 orders of magnitude slower segmental dynamics, which corresponds to a T_g up to approximately 30 K higher than bulk PDMS. These changes appear as a smooth gradient of mobility, with segmental motion gradually slowing down on approaching the particle surface [28].

In the present work we study the glass transition and molecular mobility of two series of natural rubber-silica nanocomposites. Unlike PDMS, natural rubber has no affinity for the silica nanoparticles unless a coupling agent is present [31], The silica nanoparticles were prepared *in situ* using the sol–gel method. By varying the preparation protocol, we obtained nanocomposites with identical chemical structures, but two different types of morphology: *dispersed* (with particles of approximately 10 nm diameter uniformly dispersed in the volume of the polymer, similar to the PDMS-silica series previously studied [12,13,28]) and *aggregated*, where the silica phase consists of large aggregates tens or hundreds of nanometers in diameter. Compared to the PDMS-silica and PDMS-titania systems, the interaction of the polymer chains with the particles surface is weaker-Van der Waals forces rather than hydrogen bonds; also no crystallinity is observed, simplifying the analysis. We characterize the glass transition using differential scanning calorimetry, and study the segmental and local molecular dynamics in a broad temperature and frequency range using two dielectric techniques: thermally stimulated depolarization currents and broadband dielectric spectroscopy.

2. Experimental

2.1. Materials

Two series of natural rubber-silica composites were prepared. The details of sample preparation and morphological characterization have been published elsewhere [32] and are summarized below. The silica particles were synthesized *in situ* within the polymer matrix, by hydrolysis and polycondensation of tetraethoxysilane (TEOS) in the presence of a pH-neutral catalyst.

2.1.1. First series (dispersed composites)

The natural rubber was first crosslinked, then silica nanoparticles were formed by swelling the rubber networks in TEOS followed by the hydrolysis and polycondensation reactions. This procedure is the same as the one followed for the PDMS-silica and PDMS-titania nanocomposites that were previously studied. Using transmission electron microscopy, we observed small silica nanoparticles with a diameter of *ca.* 10 nm, homogeneously dispersed in the rubber matrix [32]. The silica content was controlled by varying the swelling time, and samples with 5, 6, 9 and 11% silica by volume were prepared, referred to in the following as D-5%, D-6%, D-9% and D-11% respectively.

2.1.2. Second series (aggregated composites)

For the second series the uncrosslinked rubber was dissolved in toluene and mixed with the silica precursor; the formation of the nanoparticles was carried out in solution and the sample was then dried and finally crosslinked. The resulting composites are characterized by large silica aggregates, with a broad size distribution ranging from tens to hundreds of nanometers [32]. Samples containing 11, 16 and 18% silica by volume were studied. In the 16% silica sample, 4% of coupling agent (Si69) was added, in order to enhance the polymer-filler interactions; in this sample an aggregate morphology was again obtained with only slightly higher degree of nanoparticle dispersion. The three aggregated samples are referred to in the following as A-11%, A-16% + Si69 and A18%, respectively.

2.2. Experimental techniques

2.2.1. Differential scanning calorimetry

The calorimetric glass transition was studied using differential scanning calorimetry (DSC). Measurements were carried out in the temperature range 180–300 K, in nitrogen atmosphere using a Perkin Elmer Pyris 6 DSC. The samples, (with a weight of approx. 5 mg, in standard Al pans) were cooled from room temperature to 153 K at 10 K/min, held at this temperature for 2 min and the measurements were taken during subsequent heating at 10 K/min.

2.2.2. Thermally stimulated depolarization currents

Thermally stimulated depolarization currents (TSDC) is a dielectric technique which has been used extensively to study relaxation mechanisms in polymeric materials [33]. The sample is inserted between the plates of a capacitor and polarized by the application of an electric field E_P a temperature T_P for time t_P, which is large compared to the relaxation time of the molecular motions under investigation. With the electric field still applied, the sample is cooled to a temperature T_0 (sufficiently low to prevent depolarization by thermal excitation) and then is short-circuited and reheated at a constant rate b. The discharge current generated during heating is measured as a function of temperature using an electrometer. TSDC corresponds to measuring dielectric loss at a low frequency in the range 10^{-4}–10^{-2} Hz. It is characterized by high sensitivity and high resolving power and provides several variations to the experimental protocol which allow the separation of overlapping relaxations. TSDC measurements were carried out using a Keithley 617 electrometer in combination with a Novocontrol Quatro cryosystem and Novocontrol sample cell for TSDC measurements. Typical conditions were $E_P = 10^5$ V/m for the polarizing field, $T_P = 293$ K for the polarization temperature, $t_P = 5$ min for the polarization time, 10 K/min for the cooling rate to $T_0 = 123$ K and $b = 3$ K/min for the heating rate.

2.2.3. Dielectric relaxation spectroscopy

Segmental and local molecular dynamics of the polymer chains were studied using dielectric relaxation spectroscopy (DRS). Measurements were carried out in the frequency range 10^{-2}–10^6 Hz and temperature range 143–313 K with a Novocontrol Alpha analyzer. The temperature was controlled to better than 0.1 K with a Novocontrol Quatro cryosystem.

3. Results

3.1. Calorimetric glass transition

Using differential scanning calorimetry, a single glass transition at about 210 K is observed for neat natural rubber and both series of composites (Fig. 1). The glass transition temperature, heat capacity

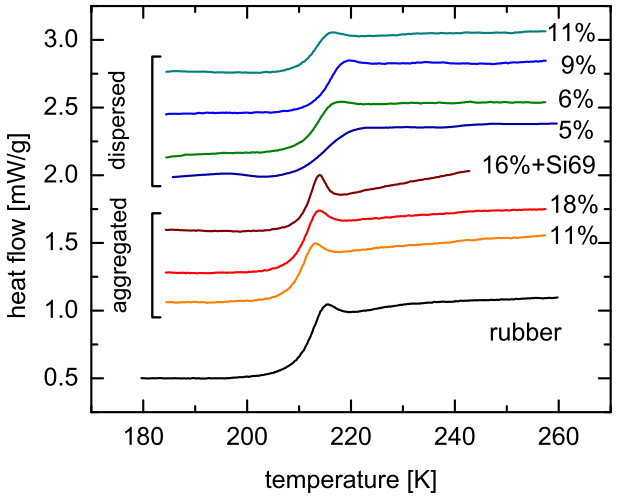

Fig. 1. DSC thermograms in the region of the glass transition for the neat natural rubber and the aggregated and dispersed composites.

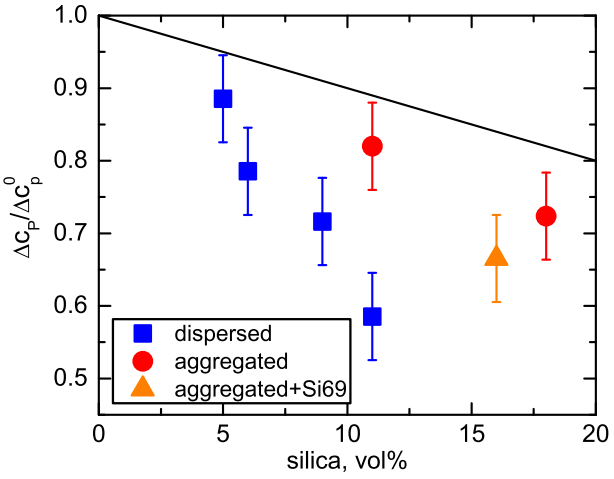

Fig. 2. Heat capacity increment, normalized by the value for the neat natural rubber, as a function of silica volume fraction. The solid line shows the decrease expected simply due to the reduced volume fraction of rubber.

increment and transition width are shown in Table 1. The silica nanoparticles only slightly affect the calorimetric glass transition temperature. For the dispersed nanocomposites, T_g increases 3–4 K compared to that of the neat rubber, with no systematic dependence on silica content. The aggregated nanocomposites, on the other hand, show the same (or marginally lower) T_g as the neat rubber. For both series of composites, the heat capacity increment, Δc_P, decreases with increasing silica content.

Fig. 2 shows Δc_P for the two series of composites. For the dispersed composites, the Δc_P decrease is significantly larger than what can be accounted for by the lower fraction of polymer in the composites, while for the aggregated composites Δc_P is close (though still less) than the expected values. A similar excess decrease in Δc_P has been observed for nanocomposites as well as for semicrystalline polymers [14]. Taking Δc_P as a measure of the amount of polymer which participates in the glass transition, this decrease is often discussed in terms of an immobilized layer of polymer around the filler particles, or crystallites, respectively. The fraction of immobilized polymer can then be calculated by

$$x_{\mathrm{im}} = 1 - \frac{\Delta c_p}{\Delta c_p^0 (1 - w_{\mathrm{SiO_2}})} \qquad (1)$$

where $\Delta c_P{}^0$ is the heat capacity increment of the neat rubber and $w_{\mathrm{SiO_2}}$ the weight fraction of silica. The values of χ_{im} thus obtained are shown in Table 1. For the dispersed nanocomposites, they range from 5 to 30% increasing with increasing silica content. Assuming homogeneously dispersed particles of 10 nm diameter, this corresponds to an immobilized interfacial layer of 2–3 nm. For the aggregated nanocomposites with similar silica volume fractions, only a minimal fraction (1–2%) of polymer is immobilized; however adding coupling agent increases the surface to volume ratio resulting in increased χ_{im} in sample A-16 + Si69.

Table 1
Parameters of calorimetric glass transition: glass transition temperature, heat capacity increment, transition width, and fraction of immobilized polymer calculated according to eq. (1).

Sample	T_g [K]	Δc_p [J/(g K)]	$\Delta\epsilon$ [K]	χ_{im}
Neat rubber	210.7	0.550	4.9	0.0
D-5%	215.2	0.487	5.1	0.05
D-6%	216.2	0.432	6.6	0.13
D-9%	214.8	0.394	5.6	0.16
D-11%	214.2	0.322	5.5	0.29
A-11%	209.5	0.451	3.8	0.01
A-18%	210.2	0.398	3.7	0.02
A-16% + Si69	209.8	0.366	3.3	0.12

3.2. Thermally stimulated depolarization currents

Fig. 3 shows TSDC thermograms in the region of the glass transition. For the neat rubber and all composites, a sharp peak is observed around the glass transition temperature, corresponding to the segmental α relaxation of the polymer matrix. At higher temperatures (not shown), a broad and intense peak is observed due to interfacial polarization, *i.e.*, accumulation of charges at the interfaces between the matrix and filler.

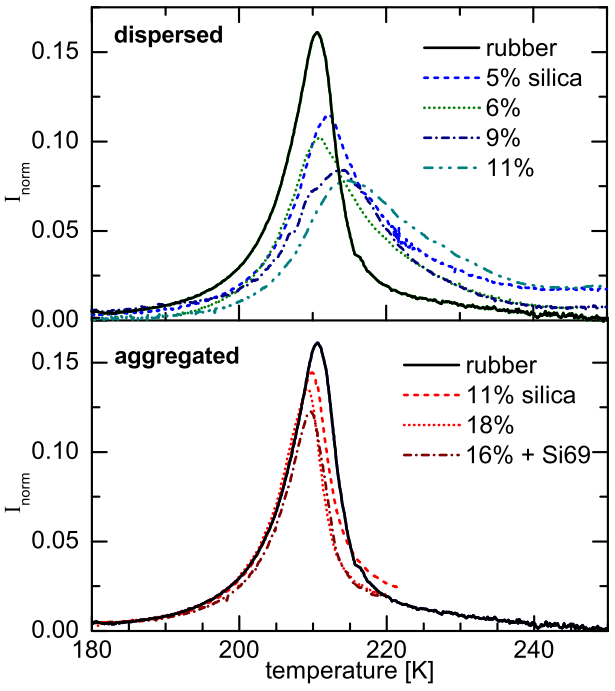

Fig. 3. TSDC thermograms in the region of the glass transition. In the aggregated composites, the α peak broadens considerably indicating a fraction of polymer with higher T_g.

Table 2
Parameters of the segmental α relaxation from TSDC: Peak temperature, dielectric increment normalized by the polymer volume fraction, and transition width.

Sample	T_α [K]	$\Delta\epsilon_{norm}$	ΔT [K]
Neat rubber	210.6	0.09	7.5
D-5%	210.9	0.08	13.1
D-6%	212.4	0.09	12.6
D-9%	214.1	0.08	15.5
D-11%	214.2	0.11	21.3
A-11%	209.3	0.09	6.9
A-18%	210.7	0.08	7.1
A-16% + Si69	210.0	0.10	7.6

The temperature T_α of the segmental relaxation peak (Table 2) is usually found to be in good agreement with the calorimetric glass transition temperature [33]. Indeed, the two temperatures are very close (with the exception of D-5% and D-9% where a small difference of *ca.* 3 K exists). Glass transition temperatures from TSDC and DSC follow the same trends: a small systematic increase compared to the neat rubber for the dispersed silica and no change or a marginal decrease in the case of aggregated silica.

From the total charge recorded during depolarization for the α relaxation (total charge is proportional to the area of the TSDC peak), the dielectric increment $\Delta\epsilon_\alpha$ of the relaxation was calculated, representing the contribution of the segmental process to the static dielectric constant. Values of $\Delta\epsilon_\alpha$, normalized by the volume fraction of polymer in each composite, are shown in Table 2. The normalized relaxation strength is within the range 0.08–0.11 for the neat rubber and both series of composites, showing no systematic variation with silica content or morphology. Notably, there is no decreasing trend of $\Delta\epsilon_\alpha$ with increasing silica content, as was the case for the heat capacity increment.

The shape of the α relaxation peak, reflecting the distribution of segmental relaxation times, shows very different behavior for the two series of composites. For the aggregated composites the peak shape is identical to that of the pure rubber. For the dispersed composites, the peak broadens significantly on the high-temperature side. This broadening increases with increasing silica content. This suggests heterogeneous dynamics, *i.e.* that there are regions of the material, presumably around the silica nanoparticles, with a glass transition temperature up to *ca.* 20 K higher than the bulk polymer. Again, this differs from the calorimetric glass transition, where no broadening was observed.

3.3. Dielectric relaxation spectroscopy

Fig. 4 shows representative dielectric spectra for the two series of nanocomposites. At low temperatures we follow two local relaxations, γ and β, of which the γ process in only present in the composites and not the neat natural rubber. At higher temperatures, we observe the much stronger α relaxation, associated with the glass transition and finally at low frequencies and high temperatures, an increase in the dielectric loss due to dc conductivity and interfacial polarization. We fit the dielectric spectra using the Havriliak–Negami (HN) function [34]

$$\epsilon^*(f) = \frac{\Delta\epsilon}{\left[1+(if/f_0)^\alpha\right]^\beta} \quad (2)$$

for each relaxation process, where f_0 is a characteristic frequency related to the frequency of maximum loss of the relaxation (f_{max}), $\Delta\epsilon$ is the dielectric strength or contribution of the relaxation to the static dielectric constant, and α and β are shape parameters.

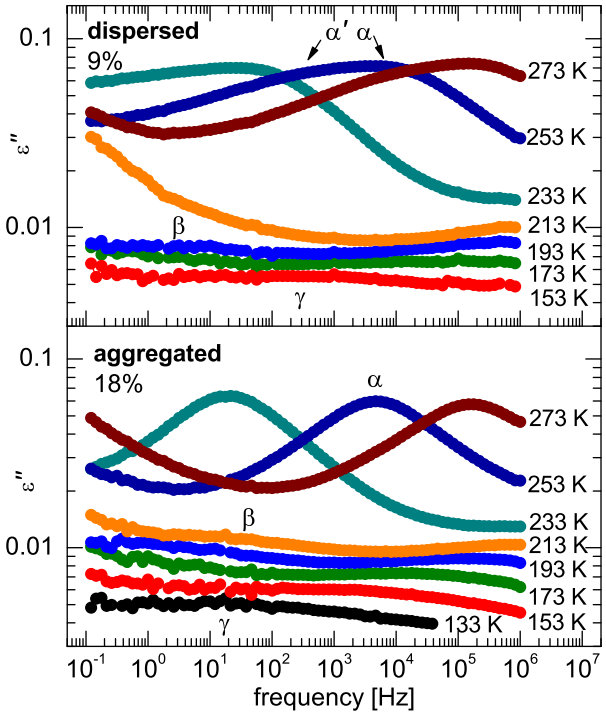

Fig. 4. Representative dielectric loss spectra for the dispersed and aggregated composites.

3.3.1. Segmental relaxation processes

Natural rubber, is primarily composed of *cis*-1,4-polyisoprene (PI) chains. *cis*-PI is a type-A polymer, having a dipole moment component parallel to the chain backbone. Therefore, uncrosslinked natural rubber shows a low-frequency dielectric relaxation (normal mode relaxation) corresponding to the motion of the chain's end-to-end vector. When the polyisoprene chains are crosslinked, the normal mode relaxation is suppressed, and only a small, broad contribution at low frequencies remains, due to the end-to-end relaxation of dangling chain ends [35]. Ortiz-Serna et al. studied the segmental relaxation of sulfur-crosslinked natural rubber, with a somewhat different curing recipe than the one used herein [36]. They found an asymmetric segmental relaxation, broad on the low-frequency side, which could be fit by a sum of two.

Havriliak–Negami functions, and attributed this behavior to the presence of the fatty acids which are part of the curing recipe.

Fig. 5 shows dielectric loss spectra for the neat natural rubber and the two series of composites at 253 K, in the frequency range of the α relaxation. The neat natural rubber shows a single, skewed dielectric loss peak, broader on the low-frequency side. As in Ref. [36], the α relaxation cannot be fitted by a single HN function. Here the excess dielectric loss at low frequencies does not take the form of a distinct shoulder, perhaps because of the lower sulfur amount in the present samples (leading to a lower degree of crosslinking compared to Ref. [36]). Although it is technically possible to fit the segmental relaxation with two HN functions, we obtained a more accurate fit, with three fewer adjustable parameters, using a single HN function plus a power law.

In the dispersed nanocomposites, a shoulder (α' process) appears on the low-frequency side of the segmental process. The shoulder is centered at a frequency roughly 2–3 orders of magnitude slower than the main α peak, and its intensity increases systematically with increasing silica content. On the other hand, for the aggregated nanocomposites, no shoulder appears and the shape of the α relaxation is identical to that of the neat rubber. This

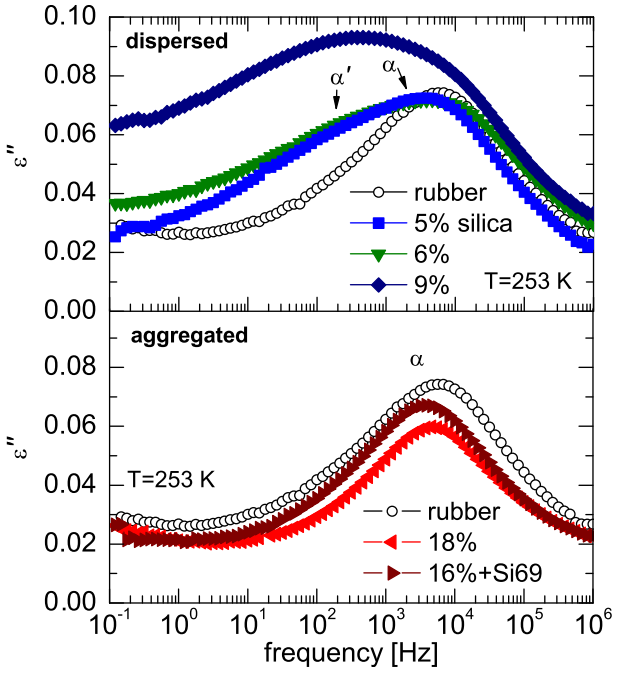

Fig. 5. Comparison of dielectric loss spectra of the dispersed and aggregated composites at 253 K.

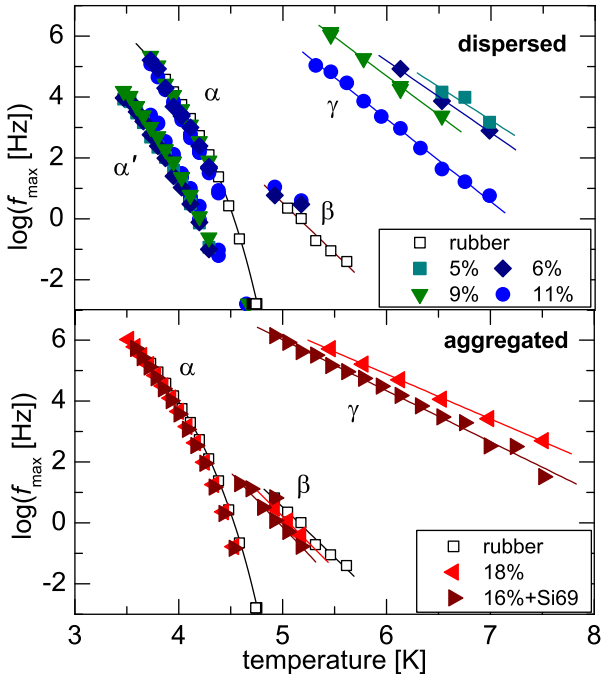

Fig. 6. Relaxation frequencies for the segmental α and α' and secondary β and γ relaxations.

behavior mirrors the results of the TSDC measurements. Landry et al. [37] have observed a similar low-frequency shoulder on the dielectric α loss peak of polyvinyl acetate filled with finely distributed sol–gel silica particles, which is absent in the same polymer filled with fumed silica having an aggregated structure.

Although the α' process is in a similar frequency range as the slow α' process observed by Ortiz-Serna et al. for neat natural rubber, its origin is clearly different. In the dispersed series of composites, the silica nanoparticles were synthesized *in situ* in the already crosslinked rubber, using the chemically mild and low-temperature sol–gel process. Therefore, the chemical structure of the natural rubber in the dispersed composites is identical to that of the neat rubber. For the aggregated composites, a small difference in crosslink density is observed, because vulcanization is carried out in the presence of the silica particles[32]. Therefore, the low-frequency contribution observed by Ortiz-Serna et al. corresponds to the slight low-frequency broadening of the α process in the neat rubber and the aggregated composites. In the dispersed composites, the *additional* low-frequency shoulder is assigned to slow segmental relaxation presumably near the silica surface. In agreement with the TSDC results, in the dispersed nanocomposites there is a fraction of polymer, presumably close to the polymer-filler interface, which relaxes slower than bulk natural rubber. For the aggregated nanocomposites, due to the low surface-to-volume ratio, no such effect is observed and the distribution of relaxation times appears identical to that of bulk natural rubber.

In the aggregated composites, we fit the α and α' processes with the sum of two HN terms plus a power law, the latter to account for low-frequency losses observed also in the neat rubber. The values obtained for the relaxation frequencies are shown in Fig. 6. The temperature dependence of the α and α' relaxation frequencies is well described by the Vogel-Tammann-Fulcher (VTF) equation [38],

$$f_{\max} = f_0 \exp\left(-\frac{DT_0}{T - T_0}\right) \tag{3}$$

characteristic of cooperative relaxations. f_0 and T_0 are temperature-independent empirical parameters. D, the so-called "strength parameter", quantifies the deviation from Arrhenius temperature dependence; within the strong-fragile classification of liquids, larger D corresponds to less fragile, or more Arrhenius-like, behavior. VTF fit parameters for the α and α' processes are shown in Table 3. The interfacial α' process has significantly larger strength parameter D, *i.e.* more Arrhenius-like behavior, than the bulk α process. This behavior was also observed for the slow interfacial relaxation in PDMS-silica and PDMS-titania nanocomposites [13,27,28]

The relaxation strengths of the α and α' processes, $\Delta\epsilon_\alpha$ and $\Delta\epsilon_{\alpha'}$ respectively, (Fig. 7) have considerable uncertainty due to the indistinct shape of the loss peak and the number of fit parameters involved. The relaxation strength of the α process decreases with increasing silica content and is relatively temperature independent, while that of the α' process decreases with increasing temperature and increases with increasing silica content and therefore increasing particle surface area. Since $\Delta\epsilon_\alpha$ is approximately constant with temperature in the neat rubber, this suggests that the amount of interfacial polymer, which gives rise to the α' process, decreases with increasing temperature similar to the PDMS-silica nanocomposites previously studied [12]. Assuming homogeneously dispersed particles of 10 nm diameter, this corresponds to an interfacial layer of 2–4 nm, in rough agreement with the DSC results.

Table 3
Activation parameters for the α, α' and γ processes. For the α' process the value of $\log f_0$ was fixed to 12.0.

Sample	α Process			α' Process			γ Process	
	$\log f_0$	D	T_0 [K]	$\log f_0$	D	T_0 [K]	$\log f_0$	E_a [eV]
Neat rubber	11.3	8.5	167	–	–	–	–	–
D-5%	11.5	9.0	167	12.0	17.6	146	18.6	0.44
D-6%	11.4	8.5	169	12.0	18.0	145	19.4	0.47
D-9%	12.3	9.2	166	12.0	17.0	147	20.0	0.51
D-11%	12.0	10.2	160	12.0	17.4	147	19.6	0.54
A-18%	11.5	9.0	169	–	–	–	14.4	0.33
A-16% + Si69	11.5	8.7	170	–	–	–	13.7	0.29

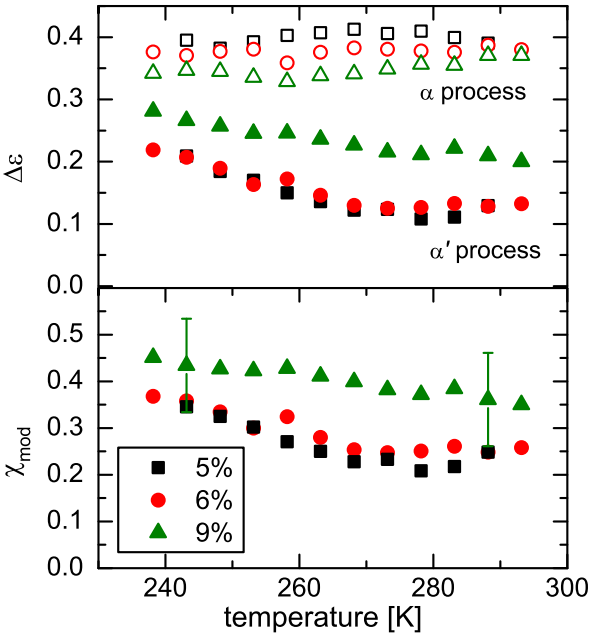

Fig. 7. Temperature dependence of the dielectric strength of the α and α' segmental processes in the dispersed composites.

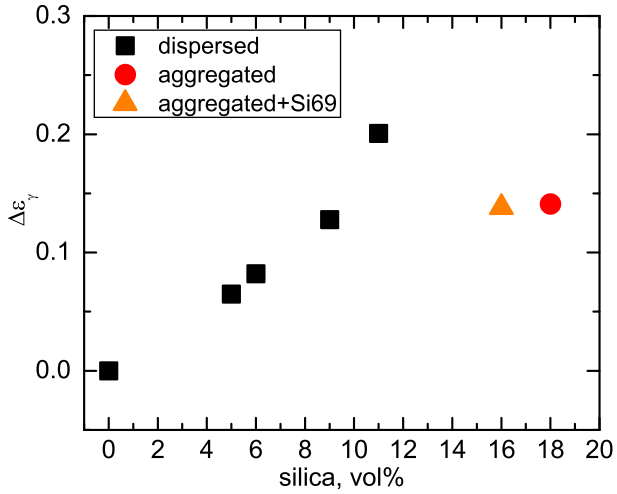

Fig. 8. Dielectric strength of the secondary γ process as a function of silica content.

3.3.2. Local relaxation processes

Both the neat rubber and the two series of composites show a weak local β relaxation, with no systematic dependence on silica content or morphology. It has an Arrhenius temperature dependence, with a rather large activation energy of *ca.* 0.65 eV and pre-exponential factor of $\log f_0 = 17-18$. The origin of this process is not entirely clear. In linear cis-1,4-polyisoprene, a very weak secondary relaxation of the Goldstein–Johari variety (*i.e.*involving motions of the entire molecule and associated with the precursor to segmental motion) has been observed [39]. This relaxation is however 2–3 orders of magnitude faster than our β process and its activation energy and pre-exponential factor much lower. We conjecture that the β process could be associated with polar groups incorporated into the molecular structure by the vulcanization process, such as carbon-sulfur bonds at the crosslinks as well as side groups formed by reaction with the vulcanization activators. Ortiz-Serna et al. [36] did not observe a β process in vulcanized natural rubber, possibly due to the differences in the vulcanization package used.

The faster γ process appears in the composites of both series, but is absent in the neat natural rubber. Fig. 8.shows the relaxation strength of the process at 183 K as a function of filler content. The γ process becomes systematically stronger with increasing silica content, and is stronger for the dispersed composites compared to the aggregated composites at similar silica content. This suggests that the γ relaxation takes place at the filler surface. The activation energy, E_γ, shown in Table 3 is somewhat lower for the aggregated composites than the dispersed ones. A relaxation with very similar characteristics to the γ process was also observed in sol–gel PDMS-silica nanocomposites, attributed to local motions of silanol groups on the filler surface, with the participation of adsorbed water molecules. The γ process is likely related to the ubiquitous local relaxation observed in water-containing systems, which occurs in the same temperature range and with an activation energy similar to E_γ in the dispersed samples [40]. The difference in activation energy between aggregated and dispersed composites is probably due to the differing local environment: the filler surface is primarily silica–silica interfaces inside aggregates in the aggregated composites, as opposed to almost exclusively silica-polymer interfaces in the dispersed composites.

4. Discussion

As noted above, at first glance there seems to be an inconsistency between the results of DSC and dielectric measurements on the dispersed composites. Looking first at the DSC results, there is only a marginal increase in calorimetric T_g, but a substantial decrease in the heat capacity step. No broadening on the high-temperature side of the transition is observed, which would be expected in the case of slowing down of the interfacial dynamics. Taken in isolation, these results would seem to suggest an immobilized or glassy interfacial layer, with a thickness of a few nm, around the silica particles. In such a layer no segmental motion would presumably take place [14,41–43]. This sort of immobilized layer is discussed in detail by Sargsyan et al. [14], based on very accurate calorimetric measurements on PMMA-silica nanocomposites, also drawing parallels with the rigid amorphous layer (RAF) in semicrystalline polymers [44]. Surprisingly, this immobilized layer is not observed to devitrify even at very high temperatures [14].

On the other hand, both dielectric techniques-DRS and TSDC-suggest a qualitatively different picture. The dynamic glass transition is considerably broadened on the low frequency or high temperature side, while the total intensity of the segmental relaxation, normalized to the volume fraction of polymer, remains essentially constant with silica content. Thus there is no immobilized layer; segmental relaxation in the vicinity of the silica particles is directly observed to occur, albeit with 2–3 orders of magnitude longer relaxation time compared to the bulk. About 20–30 K higher than the bulk T_g, the interfacial layer has completely devitrified and there is no longer a glassy layer around the filler particles.

How can these two apparently contradictory pictures be reconciled? It seems that the nanoparticles affect the segmental dynamics in a way that does not correspond either to a simple shift of T_g of the bulk material or to complete immobilization of a fraction of polymer segments. Rather, qualitatively different molecular motions than those of the bulk state take place. In such a case, since dielectric and calorimetric techniques probe molecular motions in different ways, their results should not necessarily follow each other. A possible interpretation is that the segments in close proximity to the surface have fewer available conformations, and

therefore reduced configurational entropy compared to the bulk. On one hand, this would be expected to lead directly to a drop in Δc_P, without needing to invoke a glassy or immobilized layer. On the other hand, according to the Adam–Gibbs approach, and related entropy-based models of the glass transition [45], one would expect a slowing down of molecular motions, as is in fact observed using DRS and TSDC.

DSC, TSDC and DRS results all indicate that the range of the particle–polymer interaction is on the order of a few nanometers; at larger distances away from the particle surface the dynamics reverts to bulk behavior. This is consistent with an explanation in terms of intermolecular cooperativity, since the intrinsic cooperative length scale for the segmental relaxation is on the order of a few nm, decreasing with increasing temperature [46]. The particle surface induces a modification in the dynamics of the immediately adjacent polymer segments; the length scale over which the modification persists into the volume of the polymer is given by the cooperativity length [12]. The same approach has been used more generally, *e.g.* to rationalize the dynamics of molecular liquids under nanoscale confinement [47]. The small length scale of the polymer-filler interaction also explains why the dynamics of the aggregated nanocomposites, and of systems in the literature with fillers of similar length scale of tens of nanometers [8] appear unaffected by the silica phase. Of the aggregated composites, only the 16% + Si69 sample, which has a somewhat more dispersed silica phase, showed a small decrease in Δc_P, however any corresponding effect on the dielectric α relaxation of this sample, if present, was too small to be observed.

It is interesting to compare the dispersed rubber-silica samples to the PDMS-silica and PDMS-titania nanocomposites studied previously [12,13,27,28]. In the PDMS-silica series, the silica nanoparticles were prepared using an identical process to the dispersed samples herein and have very similar size, surface chemistry and dispersion characteristics, while titania nanoparticles are somewhat larger but also well dispersed. Though crystallization of PDMS must also be taken into account, the main characteristics of all three systems are the same: significantly reduced heat capacity step, and slowed down segmental relaxation in an interfacial region with a thickness of a few nm. The slow interfacial dynamics also exhibit lower fragility, *i.e.*, more Arrhenius-like behavior compared to the bulk. The main difference between the three systems lies in the magnitude of the change in relaxation times (Fig. 9): in the PDMS-silica nanocomposites, where the polymer chains interact strongly with the silica surface through hydrogen bonds, the slowing sown of the dynamics is much more pronounced, at 3–5 orders of magnitude compared to 2–3 for natural rubber. In the PDMS-titania system, the polymer-filler interaction is even stronger than that between PDMS and silica, leading to even more pronounced slowing down of segmental motions in the interfacial layer [13].

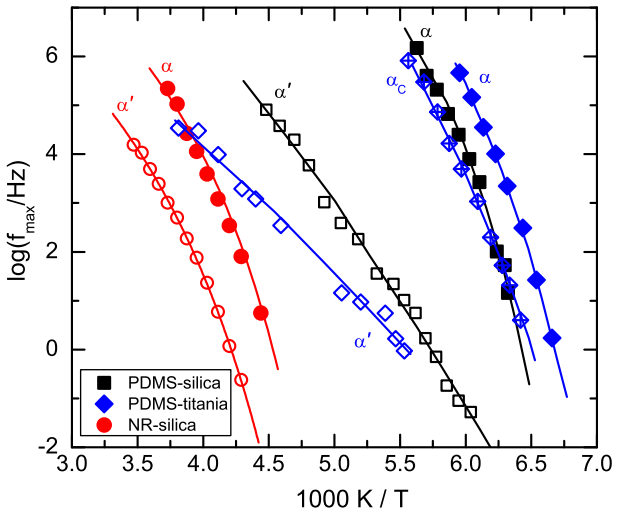

Fig. 9. Comparison of segmental relaxation times in NR-silica (dispersed, 9vol% silica), PDMS-silica (11vol% silica, data from [28]) and PDMS-titania (15.3vol% silica, data from [13]) nanocomposites. Filled symbols: bulk α process, empty symbols: interfacial α' process. In the PDMS-titania nanocomposites the additional, intermediate process, α_C, corresponds to segments restricted between crystalline regions.

5. Summary

The effect of silica nanoparticles on the glass transition and molecular mobility of natural rubber networks was studied using differential scanning calorimetry and dielectric techniques. The filler particles were synthesized *in situ* using the sol–gel technique which allows for control of the particle dispersion. For composites containing aggregates of nanoparticles with characteristic sizes of tens to hundreds of nanometers, no significant effects were observed on molecular mobility. For finely distributed 10 nm nanoparticles, a fraction of polymer shows restricted segmental mobility, characterized by slower segmental relaxation times by 2–3 orders of magnitude and reduced heat capacity increment at T_g compared to bulk behavior.

Both calorimetric and dielectric techniques indicate that the range of the polymer-filler interaction is of the order of a few nanometers, consistent with an explanation in terms of intermolecular cooperativity. A decrease in the heat capacity increment is often interpreted as a persistent immobile glassy layer or rigid amorphous fraction of polymer around the filler particles. However, both dielectric techniques show that the interfacial region is mobile, albeit slowed down, with relaxation times up to 2–3 orders of magnitude slower than the bulk values. The results of all three techniques can be rationalized by considering that in the interfacial region configurational entropy is reduced due to the restrictions imposed by the particle surface.

Compared to PDMS networks filled with identical silica nanoparticles, the natural rubber-silica nanocomposites show similar overall behavior. The length scale of the polymer-filler interactions is similar, but weaker polymer-filler interactions in the rubber-silica system lead to a weaker effect on the segmental relaxation times at the interface.

References

[1] Jancar J, Douglas JF, Starr FW, Kumar SK, Cassagnau P, Lesser AJ, et al. Polymer 2010;51:3321.
[2] Moniruzzaman M, Winey KI. Macromolecules 2006;39:5194.
[3] Okada A, Usuki A. Macromol Mater Eng 2006;291:1449.
[4] Bokobza L. Macromol Mater Eng 2004;289:607.
[5] Bokobza L. Polymer 2007;48:4907.
[6] Kumar SK, Krishnamoorti R. Ann Rev Chem Biomol Eng 2010;1:37.
[7] Alcoutlabi M, McKenna GB. J Phys: Condens Matter 2005;17:R451.
[8] Bogoslovov RB, Roland CM, Ellis AR, Randall AM, Robertson CG. Macromolecules 2008;41:1289.
[9] Ash BJ, Siegel RW, Schadler LS. J Polym Sci Part B: Polym Phys 2004;42:4371.
[10] Rittigstein P, Priestley RD, Broadbelt LJ, Torkelson JM. Nat Mater 2007;6:279.
[11] Hub C, Harton SE, Hunt MA, Fink R, Ade H. J Polym Sci Part B: Polym Phys 2007;45:2270.
[12] Fragiadakis D, Pissis P, Bokobza L. J Non-Cryst Solids 2006;352:4969.
[13] Klonos P, Panagopoulou A, Bokobza L, Kyritsis A, Peoglos V, Pissis P. Polymer 2010;51:5490.
[14] Sargsyan A, Tonoyan A, Dactyan S, Schick C. Eur Polym J 2007;43:3113.
[15] Harton SE, Kumar SK, Vand H, Koga T, Hicks K, Lee H, et al. Macromolecules 2010;43:3415.
[16] Tsagaropoulos G, Eisenberg A. Macromolecules 1995;28:6067.
[17] Litvinov V, Spiess H. Macromol Chem Phys 1991;192:3005.
[18] Kirst K, Kremer F, Litvinov V. Macromolecules 1993;26:975.
[19] Arrighi V, McEwen I, Qian H, Prieto M. Polymer 2003;44:6259.

[20] Matejka L, Dukh O, Kolarik J. Polymer 2000;41:1449.
[21] Berriot J, Montes H, Lequeux F, Long D, Sotta P. Macromolecules 2002;35:9756.
[22] Robertson CG, Roland CM. Rubber Chem Technol 2008;81:506.
[23] Salaniwal S, Kumar SK, Douglas JF. Phys Rev Lett 2002;89:258301.
[24] Robertson CG, Rackaitis M. Macromolecules 2011;44:1177.
[25] Kickelbick G. Prog Polym Sci 2003;28:83.
[26] Mark J. Polym Eng Sci 1996;36:2905.
[27] Klonos P, Panagopoulou A, Kyritsis A, Bokobza L, Pissis P. J Non-Cryst Solids 2011;357:610.
[28] Fragiadakis D, Pissis P, Bokobza L. Polymer 2005;46:6001.
[29] Dewimille L, Bresson B, Bokobza L. Polymer 2005;46:4135.
[30] Bokobza L, Diop AL. eXPRESS Polym Lett 2010;4:353.
[31] Bokobza L, Rapoport O. J Appl Polym Sci 2002;85:2301.
[32] Bokobza L, Chauvin JP. Polymer 2005;46:4144.
[33] Brauenlich P. Thermally stimulated relaxation in solids. Berlin: Springer; 1979.
[34] Havriliak S, Negami S. J Polym Sci C 1966;14:99.
[35] Poh BT, Adachi K, Kotaka T. Macromolecules 1987;20:2574.
[36] Ortiz-Serna P, Diaz-Calleja R, Sanchis MJ, Floudas G, Nunes RC, Martins AF, et al. Macromolecules 2010;43:5094.
[37] Landry CJT, Coltrain BK, Landry MR, Fitzgerald JJ, Long VK. Macromolecules 1993;26:3702.
[38] Vogel H. Phys Z 1921;22:645;
Fulcher GS. J Am Ceram Soc 1925;8:339;
Tammann G, Hesse W. Z Anorg Allg Chem 1926;156:245.
[39] Roland CM, Schroeder MJ, Fontanella JJ, Ngai KL. Macromolecules 2004;37:2630.
[40] Cerveny S, Alegria A, Colmenero J. Phys Rev E 2008;77:031803.
[41] Lipatov YS, Privalko VP. Polym Sci USSR 1972;14:1843.
[42] Bershtein VA, Egorova LM, Yakushev PN, Pissis P, Sysel P, Brozova L. J Polym Sci Part B: Polym Phys 2002;40:1056.
[43] Miwa Y, Drews AR, Schlick S. Macromolecules 2006;39:3304.
[44] Wunderlich B. Prog Polym Sci 2003;28:383.
[45] Adam G, Gibbs JH. J Chem Phys 1965;43:139.
[46] Donth E. The glass transition: relaxation dynamics in liquids and disordered materials, Springer series in materials science II, vol. 48. Berlin: Springer; 1998.
[47] He F, Wang LM, Richert R. Eur Phys J Spec Top 2007;141:3.